Food Chemistry 139 (2013) 963–969

Contents lists available at SciVerse ScienceDirect

Food Chemistry

journal homepage: www.elsevier.com/locate/foodchem

Analytical Methods

Development of electrochemical biosensor with nano-interface for xanthine sensing – A novel approach for fish freshness estimation

Kavitha Thandavan [a], Sakthivel Gandhi [a], Swaminathan Sethuraman [a], John Bosco Balaguru Rayappan [b], Uma Maheswari Krishnan [a,*]

[a] Centre for Nanotechnology & Advanced Biomaterials, School of Chemical & Biotechnology, SASTRA University, Thanjavur 613 401, TamilNadu, India
[b] Centre for Nanotechnology & Advanced Biomaterials, School of Electrical & Electronics Engineering, SASTRA University, Thanjavur 613 401, TamilNadu, India

ARTICLE INFO

Article history:
Received 10 July 2012
Received in revised form 4 December 2012
Accepted 2 February 2013
Available online 15 February 2013

Keywords:
Xanthine oxidase
Amperometry
Iron oxide
Xanthine
Biosensor
Fish

ABSTRACT

Highly sensitive, selective and mediator-free electrochemical biosensor with nano-interface for sensing xanthine using xanthine oxidase (XOx) has been developed. Towards the preparation of nano-interface, Fe_3O_4 nanoparticles were synthesized by thermal co-precipitation method and structural, morphological characterizations were carried out using X-ray diffraction (XRD), field emission scanning electron microscope (FE-SEM) and field emission transmission electron microscope (FE-TEM) respectively. The modified electrode with the covalently linked XOx was confirmed by FT-IR. With the modified electrode as working electrode, electrochemical studies were carried out. The linear range was found to be from 0.4 to 2.4 nM. The biosensor exhibited an optimum response in less than 2 s and was not prone to interferences from ascorbic acid, urea and sucrose. The Michaelis–Menten constant (K_m) was found to be 1.3 nM. The limit of detection is found to be 2.5 pM and limit of quantification as 8.3 pM. The developed biosensor was used for the real time measurement of fish freshness.

1. Introduction

In recent past, development of biosensors for the quantitative determination of xanthine, have gained momentum because of their key role in the fields of medicine and food industries (Mao & Yamamoto, 2011; Yu Febuxostat, 2007). Quantitative detection of xanthine levels in fish food will help to estimate directly its freshness level. A variety of methods namely HPLC, spectrophotometry, electrophoresis, chemiluminescence have been used for xanthine determination. These techniques are found to be costly, time consuming and involve complex procedures (Shen, Yang and Peng, 1996). Electrochemical analysis is one of the most active research areas in the recent past as it involves various advantages namely less time, high specificity, simple procedure involved (Shen et al., 1996).

Mulchandani, Luong, and Male (1989), developed a biosensor, which utilized the fish extract, for the determination of its quality by sensing hypoxanthine. Rehak, Snejdarkova, and Otto (1994) reported a biotin-streptavidin technology based xanthine biosensor by using self-assembled phospholipid membrane. Later (Mao, Jin, Song, Yamamato, & Jin 1999) utilized carbon fibre microelectrode for in vivo measurements of oxygen, which made use of nafion and methyl viologen for the electrochemical determination of xanthine. In the year Shi et al. (2002) reported a hypoxanthine biosensor, which is able to detect the hypoxanthine levels in myocardial cells. Later, Basu, Chattopadhya, Roy Choudhury, and Chakraborty (2005) developed an amperometry-based biosensor, which can estimate the hypoxanthine in fish and meat tissue. Lawal and Adeloju (2008) reported a xanthine oxidase potentiometric sensor based on polypyrrole for sensing hypoxanthine. However, immobilisation techniques for the enzyme xanthine oxidase used in the above-mentioned reports possess disadvantages such as slow electron transfer and lack of stability.

The determination of xanthine has also been done using various mediators namely gold nanoparticles (Pingarrón, Paloma, & Aracelli, 2008), colloidal gold (Liu, Nie, Tao, & Yao, 2004), Prussian blue (Teng, Chen, Zhou, Zhao, & Lan 2010), cobalt pthalocyanin Kilinc, Erdem, Gokgunnec, Dalbasti, Karaoglan and Ozsoz (1998) and ferrocene (Arslan, Yaşar, & Kılı, 2006), which was expected to improve the rate of electron transfer process. But the use of mediators involves some disadvantages (Li et al., 2006). The mediator used should not get oxidised or reduced at the potential used for detection. So the choice of mediators becomes highly important.

In this context, use of nanomaterials can efficiently transfer the electrons and eliminate the need for redox mediators (Kumar & Chen, 2008; Pandey, Datta, & Malhotra, 2008). Nanomaterials possess high surface area and numerous active sites to which the enzymes can be tagged. Moreover, the accumulation of enzymes can be prevented. A wide range of nanomaterials had been used in the

* Corresponding author. Tel.: +91 4362 304000/677; fax: +91 4362 264120.
E-mail address: umakrishnan@sastra.edu (U.M. Krishnan).

0308-8146/$ - see front matter © 2013 Elsevier Ltd. All rights reserved.
http://dx.doi.org/10.1016/j.foodchem.2013.02.008

development of nanobiosensors. Among them metal oxides namely zirconium dioxide (ZrO_2), Zinc oxide (ZnO), Cu(I)/(II) oxides, MnO_2, TiO_2, CeO_2, SiO_2 have been reported. Nanostructured metal oxides are well known for their role on enhancing the electron transfer rate between the electrode and the enzyme (Solanki, Kaushik, Agrawal, & Malhotra, 2011). Among these, nano Fe_3O_4 has generated considerable interest due to their peculiar properties *viz* biocompatibility (Jain, Reddy, Morales, Leslie-Pelecky, & Labhasetwar, 2008), high surface area and non-toxicity along with better electron transfer. Nano iron oxide has been utilized for the development of various sensors utilising enzymes namely catalase (Thandavan, Gandhi, Sethuraman, Rayappan, & Krishnan, 2011), diamine oxidase (Shanmugam et al., 2011), cellulase, glucose oxidase, urease and lactate dehydrogenase. These sensors showed better response time, improved linear range and lower detection limit.

Xanthine is a product of degradation of nucleotides. When an organism dies, degradation of the nucleotides commences leading to progressive increase in the levels of xanthine. Quantification of this molecule therefore represents a reliable method to assess the freshness of fish. Very few reports are available in literature on sensors for Xanthine to determine fish freshness. Surendra et al. performed sensing studies on xanthine for evaluating fish freshness using *n*-NiO/PEG/ITO electrode. Similarly Devi et al. have employed XOD/ZnO/MWCNT/PANI/Pt electrode to quantify xanthine in order to evaluate the freshness of Labeo *sp.* fish. Table 1 compares the characteristics of various xanthine biosensors reported in literature.

All previous xanthine sensors have reported detection levels in the micromolar range. In the early stage of fish meat storage, only nanomolar concentration of xanthine will be produced, which in turn decreases fish freshness. The present work reports a nano-interfaced biosensor that exhibits detection in the nanomolar range and enables early detection of spoilage for the widely consumed Channa striatus (Snakehead).

Xanthine oxidase belongs to the group of redox enzymes (XOx, M.W 286,000). This biomacromolecule is architectured with one molybdenum centre, two Fe_2S_2 centres and one flavin adenine dinucleotide (FAD). It has been selected for the present investigation of xanthine sensing and hence to determine the freshness level of fish flesh. In this work Fe_3O_4 nanoparticles have been chosen as an interface between electrode and xanthine oxidase. The working electrode has been fabricated in which xanthine oxidase has been covalently linked to the iron oxide nanoparticles, which are embedded on the Au working electrode. The enzyme linking to the Fe_3O_4 prevents the aggregation of enzymes to the electrode thus providing excellent electron transfer to the electrode. Here, the electroreduction of the hydrogen peroxide, produced from the xanthine in the presence of xanthine oxidase is studied using the fabricated modified working electrode (XOx/NanoFe_3O_4/Au). The designed biosensor with nanointerface showed better performance with higher sensitivity, relatively lesser time for analysis along with a new lower detection limit.

2. Materials and methods

2.1. Reagents and materials

Iron (II) chloride, diethyl carbodiimide, xanthine, xanthine oxidase (XOx) and Nafion solution (5 wt.%) were purchased from M/s Sigma Aldrich Co, Ltd (India). Sodium dihydrogen phosphate, disodium hydrogen phosphate, iron (III) chloride, ascorbic acid, urea, sucrose were purchased from Merck (India) and used as such. All solutions were prepared using Millipore water.

2.2. Characterization techniques

The structural characterization of Fe_3O_4 nanoparticles was carried out using X-ray Diffractometer (XRD) (Model D8 Focus, Bruker, Germany) that radiates Cu K_α of wavelength 1.5418 Å at 2θ range between 20° and 70°. Surface morphological information of Fe_3O_4 nanoparticles was obtained using Field Emission Scanning Electron Microscopy (FE-SEM) (Model JSM 6701F, JEOL, Japan). The particle size and morphology of iron oxide nanoparticles were characterised using Field Emission Transmission Electron Microscopy (FE-TEM) (Model JSM 2100F JEOL, Japan). Fourier Transform Infrared (FTIR) spectra of the immobilised working electrode were taken using FTIR spectrometer (Model Spectrum 100, Perkin Elmer, USA). The exact concentration of H_2O_2 was determined by UV–Vis spectrophotometer (Model Lambda 25, Perkin Elmer, USA). Cyclic voltammetry and amperometric experiments were run using an electrochemical workstation (Model CHI600C, CH Instruments, USA).

2.3. Synthesis of iron oxide nanoparticles

Iron oxide (Fe_3O_4) nanoparticles were synthesized by co-precipitation of Fe^{2+} and Fe^{3+} aqueous solutions in presence of ammonium hydroxide, a base. This is in accord with the method reported by Kouassi, Irudayaraj, and McCarty (2005). Briefly, the source of Fe^{2+} and Fe^{3+}, namely, Iron (II) chloride and Iron (III) chloride salts were dissolved in Millipore water at a ratio of 1:2. It is then precipitated by the addition of ammonium hydroxide solution (30% v/v), at room temperature (25 °C) and at a controlled pH of 10.

Table 1
Comparison of various xanthine biosensors.

Nano-interface	Enzyme	Linear range	Sensitivity	Detection limit	Technique	Refs.
Nickel oxide	Xanthine oxidase	10–200 μM	0.6214 μA/μM cm^2	2.989 μM	Amperometry	Surendra, Singh, Agarwal, and Malhotra (2012)
ZnO/MWCNT/PANI	Xanthine oxidase	0.1–100 μM	–	0.1 μM	Amperometry	Devi, Yadav and Pundir (2012)
Pt & Pd	Xanthine oxidase	Up to 70 μM	0.39 μA/μM	1.5 μM	Amperometry	Dodevska, Horozova, and Dimcheva (2007)
–	Xanthine dehydrogenase	10–1800 μM	–	0.25 nM	Amperometry	Kalimuthu, Leimkuhler, and Bernhardt (2012)
–	Xanthine oxidase	0.1–4.98 μM	13.83 mA/M	–	Amero metry	YuanJie, Chen, ChangXiang, HongLi, and MinBo (2010)
–	Xanthine oxidase	24.5–392.0 ng	–	–	HPLC	Zhao, Cui, Di, and Li (2002)
	Xanthine oxidoreductase & xanthine dehydrogenase	5–40 μM	0.08 AU/μM	5.1 μM	HPLC	Affum (2007)
Fe_3O_4	Xanthine oxidase	0.4–2.4 nM	4.94 μA/nM	2.5 pM	Amperometry	Present work

The obtained suspensions were then heated for 35 min at 80 °C under continuous stirring. It is then centrifuged at 2800 rpm several times using water, ethanol sequentially for the removal of impurities. The sediment particles after the removal of supernatant were dried in a vacuum oven at 70 °C. The iron oxide nanoparticles thus obtained were used for further studies.

2.4. Covalent linking of xanthine oxidase (XOx) enzyme onto the Nano Fe_3O_4

In accordance with the method reported by Kouassi et al. (2005), XOx enzyme was covalently linked to Fe_3O_4 nanoparticles. Approximately, 50–70 mg of magnetic nanoparticles was taken and 1 mL of 0.1 M phosphate buffer of pH 7.4 was added. Then carbodiimide activation, was carried out using 0.5 mL of N-(3-dimethylaminopropyl)-N′-ethylcarbodiimide hydrochloride solution (0.02 g/mL in phosphate buffer) by adding it to the above mixture followed by sonication for 15 min. Finally, 10 μL of XOx (1 unit/mL) enzyme solution was added and the reaction mixture was sonicated for 30 min at 4 °C in a sonication bath. This mixture was centrifuged at 3000 rpm and the precipitates containing Fe_3O_4 bound XOx were washed sequentially with 0.1 M phosphate buffer (pH 7.4), 0.1 M Tris (pH 8.0) and 0.1 M NaCl. The product thus obtained is then used for electrochemical sensing.

2.5. Fabrication of XOx/Nano Fe_3O_4/Au electrode

To obtain a clean and reproducible surface, the gold electrode was polished with α-alumina powder of 1.0, 0.3 micron respectively using nylon polishing pads and with 0.05 micron γ-alumina powder using microcloth polishing pad. It was then ultrasonically cleaned with acetone and finally with distilled water for ten minutes each and dried in air. Then the 3 μL of the mixture of Fe_3O_4 nanoparticles tagged with XOx was pipetted out onto the surface of the working gold electrode and dried. It was then covered with the nafion membrane (0.5 wt.%) and thus the working electrode was fabricated.

2.6. Preparation of the fish extract

Channa striatus, an export quality fish was purchased from the local market for quality analysis. The fish extract was prepared as in the method reported by Nakatani, Vieira dos Santos, Pelegrine, and Evelázio de Souza (2005). Here the fish was sacrificed and the fillets of 5 g each were weighed and kept separately in the freezer at −20 °C. A fillet was then homogenised using 15 mL water and the extract was made up to 25 mL. Then centrifugation was carried out for the fish extract at 8000 rpm for 10 min. The supernatant thus obtained was filtered using a 0.2 μm membrane filter and the pure sample was isolated and used for the analysis. The experiment was carried out at room temperature.

2.7. Determination of xanthine in the fish muscle

An aliquot of the extract prepared by the above mentioned method was transferred to the cell containing 5 mL phosphate buffer. Gold electrode modified with XOx, serves as the working electrode. The other electrodes namely the reference saturated Ag/AgCl and platinum wire counter electrode were inserted into the Teflon cap and attached to the cell. A magnetic stirrer was used to stir the electrolyte solution to prevent the accumulation of charges. By using the standard addition method, 10 μL of xanthine solution of 0.4 nM was added and the corresponding increase in the peak current was noted.

3. Results and discussions

3.1. XRD data for Fe_3O_4 nanoparticles

Fig. 1 (A) shows the XRD pattern of Fe_3O_4 nanoparticles. The XRD pattern confirms the polycrystalline nature of the iron oxide nanoparticles with cubic spinel structure (Cheng et al., 2005). The characteristic peak positions obtained are found to be in agreement with JCPDS [89-0950] and are indexed to (220), (311), (400), (422) and (511) respectively. The obtained patterns agree well with the standard magnetite (Fe_3O_4) XRD patterns.

3.2. Morphology of Fe_3O_4 nanoparticles

FE-SEM and FE-TEM were used to study the particle size, shape and surface morphology of as-synthesized Fe_3O_4 nanoparticles and are shown in Fig. 1(B and C). The micrograph obtained from FE-SEM shows the uniform Fe_3O_4 nanoparticles of spherical morphology with the size ranging from 20–30 nm. From transmission electron micrograph, one can observe the crystallite nature of Fe_3O_4 rather than a spherical shape with the size ranging from 20–30 nm. The SAED (Fig. 1(D)) pattern confirms the crystalline nature of the sample.

3.3. FTIR spectroscopy for confirmation of immobilisation

Fig. 1(E) shows the FTIR spectra of (a) iron oxide nanoparticles and (b) XOx-tagged iron oxide nanoparticles. The characteristic band at 580 cm^{-1}, which appears in both spectra for iron oxide and XOx tagged iron oxide, corresponds to stretching of Fe–O bond (Chumming & Xiangqin, 2009). Additionally the XOx tagged iron oxide shows peaks at 1032 cm^{-1} corresponding to the C–N-stretch, 1632 cm^{-1} due to the amide carbonyl (amide I). The broad band at 3405 cm^{-1} which is also seen in the pristine iron oxide spectrum may be attributed to the –OH stretch. The appearance of these peaks in the XOx tagged iron oxide confirms the presence of the enzyme.

3.4. Electrochemical studies

3.4.1. Characterization of XOx/NanoFe_3O_4/Au modified electrode

Cyclic voltammogram readings obtained at a scan rate of 0.1 V/s in PBS (pH 7.4) using modified and unmodified electrodes cycled between 0.0 and 1.2 V, are shown in Fig. 2 (A). No significant redox peak was found with the bare gold electrode. Modified gold electrode coated with iron oxide nanoparticles (NanoFe_3O_4/Au) showed a characteristic peak and the same was not modified during the cycling process, which confirmed the electrochemical stability of the iron oxide nanoparticles. This clearly indicates that the influence of iron oxide nanoparticles in enhancing the current. This also confirmed the fact that the Fe_3O_4 nanoparticles can effectively shuttle electrons from the XOx to the gold electrode.

Further on addition of 0.4 nM of xanthine to the modified XOx/NanoFe_3O_4/Au nanobio electrode, a well defined reduction peak appears at +0.5 V. This may be attributed to the following reaction mechanism:

$$\text{Xanthine} + O_2 + 2H_2O \xrightarrow{XOD} +2H_2O_2 + \text{Uric acid}$$

$$2H_2O_2 \rightarrow 2H^+ + 2e^- + O_2$$

The potential interferent uric acid is overcome by cast-coating nafion film over the designed sensor (Mao & Yamamoto, 2000).

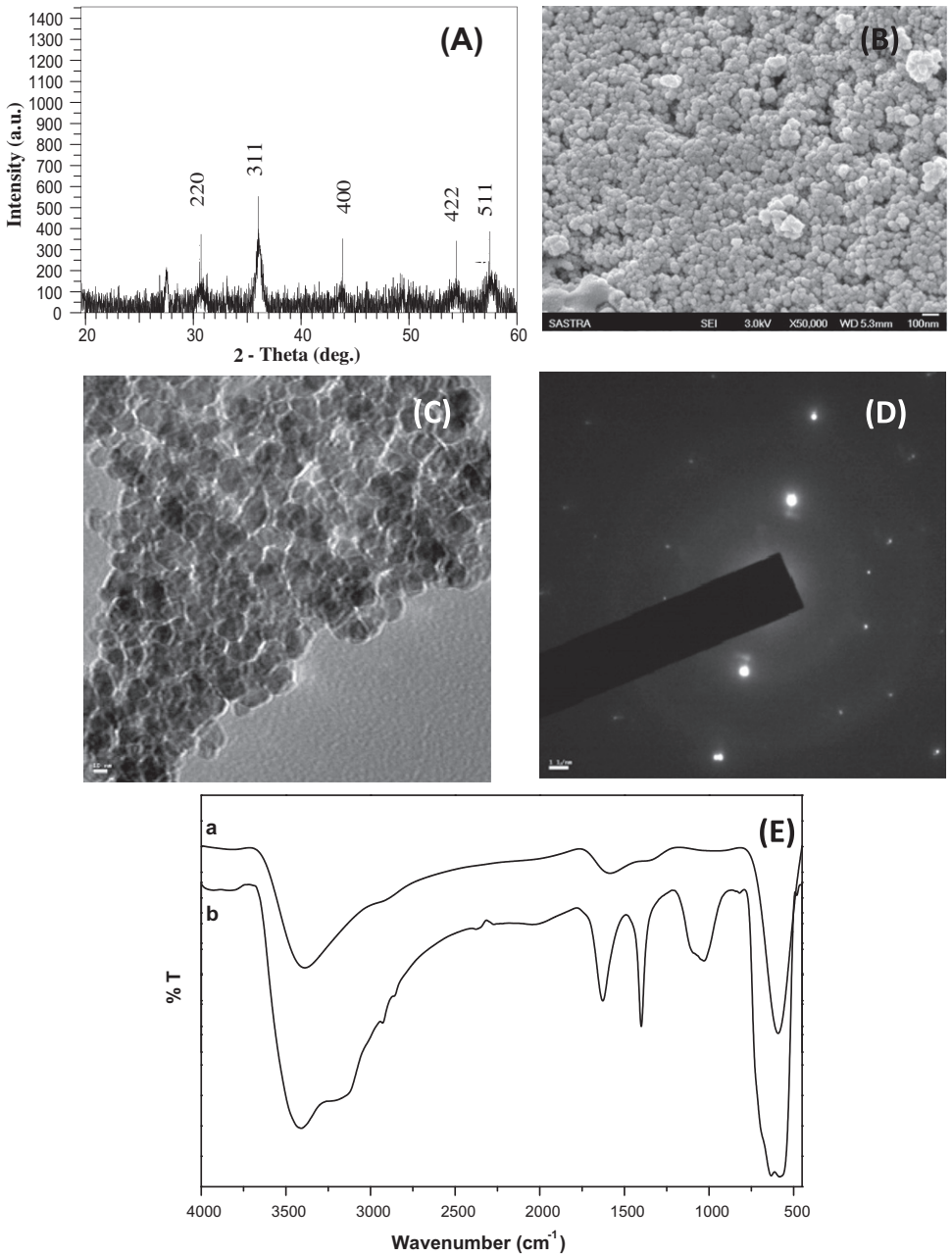

Fig. 1. XRD pattern of Fe_3O_4 nanoparticles (A),(a) FE-SEM (B), FE-TEM (C), SAED images (D) of the as-synthesized iron oxide nanoparticles and FTIR (E) of the as-synthesized (a) and XOx enzyme tagged (a) iron oxide nanoparticles.

3.4.2. Effect of scan rate on the XOx–Fe_3O_4 modified gold electrode on the electrocatalytic properties and charge transfer kinetics

The sensitivity of the detecting system mainly depends on the potential sweep rate mainly due to kinetic factors of the electrode process and instrumental limitations. Hence for its determination, the cyclic voltammograms were taken for the XOx/NanoFe_3O_4/Au modified electrode in the presence of 0.4 nM xanthine at various scan rates *viz* 0.01–0.1 V/s in a cell containing 5 mL of 0.1 M phosphate buffer (pH 7.4) are shown in Fig. 2(B). The CV patterns were recorded in a stirred solution. Both the redox peak currents and peak to peak separations increased with increasing the scan rate.

The peak currents increased linearly with the scan rate with the correlation coefficient of 0.99 suggesting this as a surface controlled process. The peak currents are directly proportional to the scan rates in the range from 0.01 to 0.1 V/s (Fig. 2(C)), consistently with thin layer electrochemical behaviour. Additionally the slope of a log (peak current) versus log (scan rate) plot (Fig. 2(D)) for the XOx/NanoFe_3O_4/Au electrode was found to be close to 1, as for the redox processes that involved surface bound species. These results confirmed that the iron oxide nanoparticles are excellent transporters of electrons between the enzyme and the electrode surface.

The surface coverage of the enzyme xanthine oxidase on the iron oxide glassy carbon electrode was estimated according to the following equation Brown Anson model (Dhyani, Ali, Pandey, Malhotra, & Sen, 2012)

$$I_p = \frac{n^2F^2\upsilon A\Gamma_c}{4RT}$$

Under the condition of saturated adsorption the average surface concentration of xanthine oxidase is about 2.7256×10^{-7} M/cm^2 indicating a sub-monolayer of enzyme immobilised on the iron

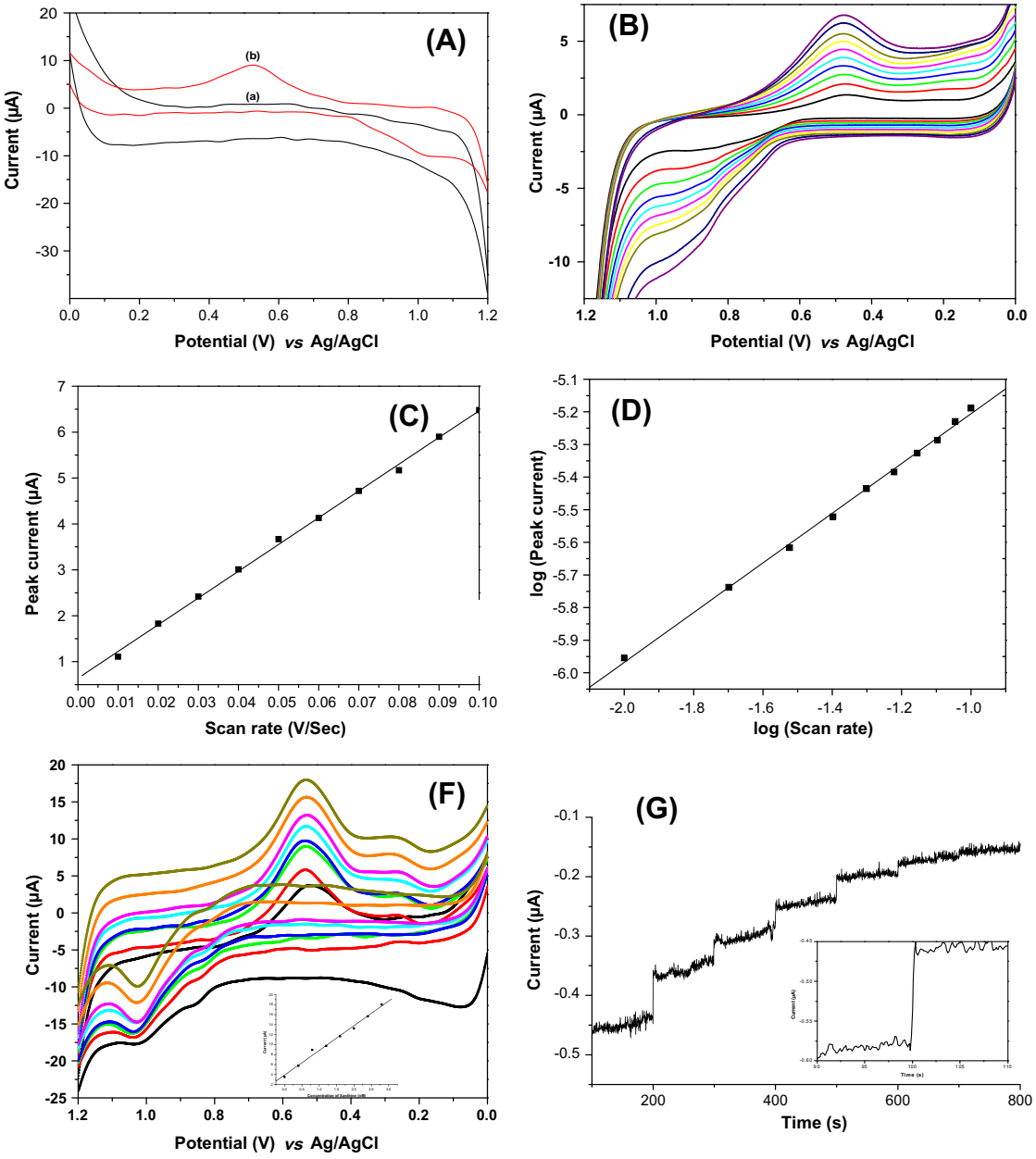

Fig. 2. Cyclic voltammogram (A) obtained in the absence (a) and in the presence (b) of Fe_3O_4 nanoparticles in the presence of 0.4 nM xanthine in a 5 mL cell containing 0.1 M phosphate buffer (pH 7.4), Cyclic voltammogram (B) obtained with the electrode modified with iron oxide at different scan rates (0.01–0.1 V/s) in a 5 mL cell containing 0.1 M phosphate buffer (pH 7.4), Calibration plots (C) drawn from the scan rate studies, Peak current *vs* scan rate. Calibration plots (D) drawn from the scan rate studies as log (peak current) *vs* log (scan rate). Cyclic voltammogram (E) obtained at XOx/Nano Fe_3O_4/Au modified electrode for increasing concentrations of xanthine (0.4–2.4 nM) at a scan rate of 0.1 V/s in a 5 mL cell containing 0.1 M phosphate buffer (pH 7.4) and its inset shows the calibration plot drawn from current *vs* concentration of xanthine. Amperometric response (F) of the XOx electrode for successive addition of 0.4 nM xanthine.

oxide-Gold electrode. The plot of log I_{pc} vs log υ gives a linear relationship with correlation coefficient of 0.9991, which is close to the theoretical slope of 1, for thin layer voltammetry.

3.4.3. Effect of concentration of xanthine

Cyclic voltammograms for increasing concentration of xanthine were recorded. As the concentration of xanthine increases both the anodic and cathodic current increases. This may be due to the increased production of hydrogen peroxide. There is no peak shift observed which confirms that the enzyme XOx is well confined to the iron oxide nanoparticles.

Fig. 2(E) shows the cyclic voltammogram for the XOx–Fe_3O_4 modified gold electrode for the successive addition of 0.4 nM xanthine to the cell containing 5 mL phosphate buffer (pH 7.4). There could be two reasons for the increase in peak current namely the improved surface area and improved electron transfer pathway. Thus the synergistic influence of iron oxide nanoparticles and the existence of xanthine oxidase promotes the reduction of hydrogen peroxide. The sensitivity of the developed sensor was calculated from slope of the linear plot and was found to be 4.94 μA nM^{-1}.

3.4.4. Amperometric detection of hydrogen peroxide using XOx–Fe_3O_4 modified gold electrode

Amperometry is based on the principle that 'when a constant potential is applied between electrodes it results in the production of current'. Hence it can give the linear range and response time.

For their determination, amperometric experiments were carried at XOx NanoFe$_3$O$_4$/Au modified electrode for the successive addition of 0.4 nM xanthine at a constant potential of 0.5 V in the cell containing 5 mL of 0.1 M phosphate buffer (pH 7.4) (Fig. 2(F)). At each step, 0.4 nM xanthine was added successively. The current increased to the peak level then stabilized and this cycle was observed for every 0.4 nM xanthine addition. With increasing concentration of xanthine the amperometric response of the enzyme electrode increases. A quick response time of 2 s was observed and this is due to the nano-scale thin iron oxide layer (Lee, Lee, Jung, & Lee, 2011. The xanthine addition was found to be linear in the range of 0.4–2.4 nM.

The limit of detection was calculated using the formula LOD = $(3 \times s_b)/S$.

where s_b represents standard deviation of the blank signal and S represents the sensitivity

Limit of quantification (LOQ) is calculated as LOQ = $(10 \times s_b)$/S.where s_b represents standard deviation of the blank signal and S represents the sensitivity. The limit of detection was found to be 2.5 pM and limit of quantification as 8.3 pM. The solution was stirred with a magnetic stirrer between each addition to prevent charge accumulation at the electrode surface. Thus the iron oxide thin film on the electrode surface efficiently retains the activity of the xanthine oxidase enzyme.

Normally, the presence of diffusion barriers and possible enzyme leaching are considered as major drawbacks which leads to high response time and the problem of instability (Sassolas, Blum, & Leca-Bouvier, 2012). But here the problem is efficiently overcome by the way of using iron oxide nanoparticle and by the covalent linkage of the enzyme to the electrode. The conductivity of the nanoparticle also plays a vital role along with the homogenity of the distribution onto the electrode surface (Song, Cui, Wang, & Chen, 2009). The Michaelis–Menten constant (K_m) was found to be 1.3 nM. The low value indicates the high affinity of the enzyme to the analyte.

3.5. Interferences

The developed bioelectrode was checked for potential interferents namely ascorbic acid, urea and sucrose at physiological concentrations viz. 0.05, 1 and 1 mM using amperometric technique at a constant potential of 0.5 V. These interferents are chosen as these are capable of interfering at this potential. It is very clear from the graph that only the addition of xanthine shows an increased value of current and subsequent addition of ascorbic acid, urea and sucrose does not show any increase in current. The results clearly showed the developed modified electrode is less prone to the interferents. This can be attributed to the nafion membrane which allows only selective molecules to penetrate and react with the xanthine. The results obtained are shown in the Fig. 3.

3.6. Stability and reproducibility

The stability of the developed electrode was checked for a period of two weeks. The modified electrode was stored in a phosphate buffer solution of pH 7.4 at room temperature. The stability is calculated using the formula

$$\%\text{Stability} = 100 - \left[\frac{I_n - I_o}{I_o} \times 100\right]$$

where I_0 is the obtained current in first day and I_n is the obtained current in 'n' day

The sensor exhibited a stable current for a period of 11 days and retained about 80% activity. The stability may be due to the good interaction between the iron oxide nanoparticles and the enzyme.

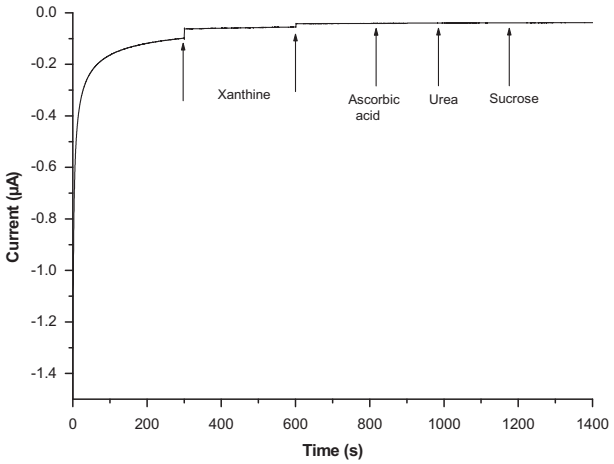

Fig. 3. The effect of potential interferents (sucrose, urea, ascorbic acid) on the XOx/Nano Fe$_3$O$_4$/Au modified electrode in a cell containing 0.4 nM xanthine.

The repeatability of the electrode was checked by performing 8 repetitive measurements and the relative standard deviation was found to be 2%, which confirmed good repeatability. The reproducibility of response between electrodes was found to be 8% RSD.

3.7. Application

The homogenised filtrate of the fish fillet was added to the cell containing 5 mL of phosphate buffer and the solution was stirred with a magnetic stirrer. When the solution became quiescent, the amperometry was set to run and thus the current was obtained for the sample. The experiment was carried out continuously for the period of 14 days from the day of the fish being sacrificed. Linearity was obtained for the first 7 days (Fig. 4), after which the linearity was found to be lost. The experiment was repeated for $n = 3$ and the standard deviations were found. Table 1 compares the characteristics of various xanthine biosensors reported in literature. When compared to other xanthine biosensor, only Fe$_3$O$_4$ based xanthine biosensor showed considerable change in current for nanomolar concentration of xanthine.

Table 2 shows the results obtained in fish samples stored at different periods and then the content of xanthine was determined. It was observed that the concentration of xanthine increases with the

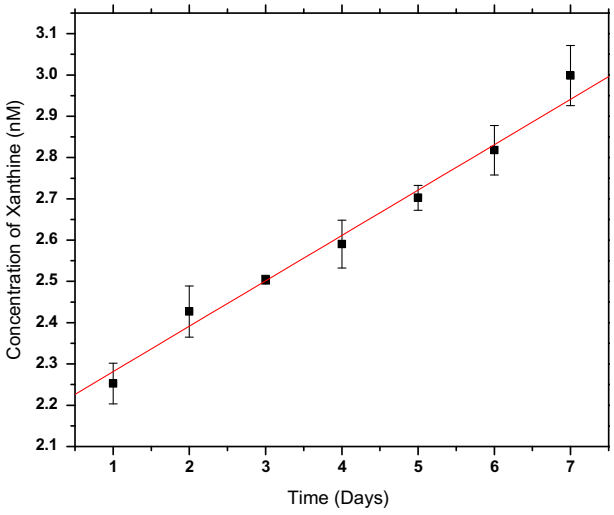

Fig. 4. Amperometric determination of changes in the levels of xanthine in fish samples over a period of time using the developed nanobiosensor.

Table 2
Determination of xanthine in fish samples using the developed biosensor for different periods of storage.

Samples	Time (h)	Concentration of xanthine (nM)
F1	24	2.2525 ± 0.0492
F2	48	2.4269 ± 0.0621
F3	72	2.5038 ± 0.0156
F4	96	2.5904 ± 0.0579
F5	120	2.7025 ± 0.0303
F6	144	2.8179 ± 0.0600
F7	168	2.9987 ± 0.0730

time of sample storage. The experiments were carried out in triplicate and their average values are tabulated.

4. Conclusions

A novel xanthine biosensor utilising nanoscale islands of iron oxide has been developed. The XOx tagged nano Fe_3O_4 modified gold electrode showed an enhanced electron transfer rate and hence the enhanced sensitivity. The detection limit was found to be 0.4 nM with a quick response time of 2 s. The linear range was found to be 0.4–2.4 nM. Thus the designed biosensor offered a lower detection limit and quick response time. This biosensor was found to be highly reproducible and stable and is free of interferences. This biosensor can detect the levels of xanthine in the fish samples and thus it can directly measure the freshness of fish.

Acknowledgements

The authors are grateful to the Department of Science and Technology (DST/TSG/PT/2008/28) for the financial support and the Drugs & Pharmaceutical Research Programme, DST for providing the FE-TEM (VI-D&P/267/08-09/TDT). We also thank SASTRA University, Thanjavur for the infrastructural support.

References

Affum A. O. (2007). Determination of xanthine and uric acid in xanthinuric urine and extracellular fluid of porcine endothelial cells of the pulmonary artery by high performance liquid chromatograpy. M.S. Thesis, University of Florida, 1-107.

Arslan, F., Yaşar, A., & Kılı, E. (2006). An amperometric biosensor for xanthine determination prepared from xanthine oxidase immobilized in polypyrrole film. *Artificial Cells, Blood Substitutes, and Immobilization Biotechnology, 34*, 113–128.

Basu, A. K., Chattopadhya, P., Roy Choudhury, U., & Chakraborty, R. (2005). Development of an amperometric hypoxanthine biosensor for determination of hypoxanthine in fish and meat tissue. *Indian Journal of Experimental Biology, 43*, 646–653.

Cheng, F. Y., Su, C. H., Yang, Y. S., Yeh, C. S., Tsai, C. Y., Wu, C. L., et al. (2005). Characterization of aqueous dispersions of Fe(3)O(4) nanoparticles and their biomedical applications. *Biomaterials, 26*, 729–738.

Chumming, J., & Xiangqin, L. (2009). Electrochemical synthesis of Fe_3O_4–PB nanoparticles with core–shell structure and its electrocatalytic reduction toward H_2O_2. *Journal of Solid State Electrochemistry, 13*, 1273–1278.

Devi, R., Yadav, S., & Pundir, C. S. (2012). Amperometric detection of xanthine in fish meat by zinc oxide nanoparticle/chitosan/multiwalled carbon nanotube/polyaniline composite film bound xanthine oxidase. *Analyst, 137*. 754–749.

Dhyani, H., Ali, M. A., Pandey, M. K., Malhotra, B. D., & Sen, P. (2012). Electrophoretically deposited CdS quantum dots based electrode for biosensor application. *Journal of Materials Chemistry, 22*, 4970.

Dodevska, T., Horozova, E., & Dimcheva, N. (2007). Biosensor for xanthine with improved sensitivity and detection limit. *Bulgaria Scientific Papers, 35*, 37–44.

Jain, T. K., Reddy, M. K., Morales, M. A., Leslie-Pelecky, D. L., & Labhasetwar, V. (2008). Biodistribution, clearance, and biocompatibility of iron oxide magnetic nanoparticles in rats. *Molecular Pharmaceutics, 5*, 316–332.

Kalimuthu, P., Leimkuhler, S., & Bernhardt, P. V., (2012). Low potential Amperometric enzyme biosensor for xanthine and hypoxanthine. *Anal. Chem.* [Epub ahead of print].

Kilinc, E., Erdem, A., Gokgunnec, L., Dalbasti, T., Karaoglan, M., & Ozsoz, M. (1998). Buttermilk Based Cobalt Phthalocyanine Dispersed Ferricyanide Mediated Amperometric Biosensor for the Determination of Xanthine. *Electroanalysis, 10*, 273–275.

Kouassi, G. K., Irudayaraj, J., & McCarty, G. (2005). Examination of cholesterol oxidase attachment to magnetic nanoparticles. *Journal of Nanobiotechnology, 3*, 1.

Kumar, S. A., & Chen, S. M. (2008). Nanostructured zinc oxide particles in chemically modified electrodes for biosensor applications. *Analytical Letters, 41*, 141–158.

Lawal, A. T., & Adeloju, S. B. (2008). Polypyrrole-based xanthine oxidase potentiometric biosensor for hypoxanthine. *Journal of Applied Sciences, 8*, 2599–2605.

Lee, H., Lee, S., Jung, S., & Lee, J. (2011). Nano-grass polyimide-based humidity sensors. *Sensors and Actuators B, 154*, 2–8.

Li, Y.-F., Liu, Z.-M., Liu, Y.-L., Yang, Y.-H., Shen, G.-L., & Yu, R.-Q. (2006). A mediator-free phenol biosensor based on immobilizing tyrosinase to ZnO nanoparticles. *Analytical Biochemistry, 349*, 33–40.

Liu, Y., Nie, L., Tao, W., & Yao, H. (2004). Amperometric study of Au-colloid function on xanthine biosensor based on xanthine oxidase immobilized in polypyrrole layer. *Electroanalysis, 16*, 1271–1278.

Mao, L., & Yamamoto, K. (2000). Amperometric on-line sensor for continuous measurement of hypoxanthine based on osmium-polyvinylpyridine gel polymer and xanthine oxidase bienzyme modified glassy carbon electrode. *Analytica Chimica Acta, 415*, 143–150.

Mao, L., Jin, L., Song, L., Yamamato, K., & Jin, L. (1999). Electrochemical microsensor for in vivo measurements of oxygen based on nafion and methyl viologen modified carbon fibre microelectrode. *Electroanalysis, 11*, 499–504.

Mao, L., & Yamamoto, K. (2011). Amperometric on-line sensor for continuous measurement of hypoxanthine based on osmium-polyvinylpyridine gel polymer and xanthine oxidase bienzyme modified glassy carbon electrode. *Analytica Chimica Acta, 415*, 143–150.

Mulchandani, A., Luong, J. H. T., & Male, K. B. (1989). Development and application of a biosensor for hypoxanthine in fish extract. *Analytica Chimica Acta, 221*, 215–222.

Nakatani, H. S., Vieira dos Santos, L., Pelegrine, C. P., Terezinha, S., Gomes, M., Matsushita, M., et al. (2005). Biosensor based on xanthine oxidase for monitoring hypoxanthine in fish meat. *American Journal of Biochemistry and Biotechnology, 1*, 85–89.

Pandey, P., Datta, M., & Malhotra, B. D. (2008). Prospects of nanomaterials in biosensors. *Analytical Letters, 41*, 159–209.

Pingarrón, J. M., Paloma, Y.-S., & Araceli, G.-C. (2008). Gold nanoparticle-based electrochemical biosensors. *Electrochimica Acta, 53*, 5848–5866.

Rehak, M., Snejdarkova, M., & Otto, M. (1994). Application of biotin-streptavidin technology in developing a xanthine biosensor based on a self-assembled phospholipid membrane. *Biosensors and Bioelectronics, 9*, 337–341.

Sassolas, A., Blum, L. J., & Leca-Bouvier, B. D. (2012). Immobilization strategies to develop enzymatic biosensors. *Biotechnology Advances, 30*, 489–511.

Shanmugam, S., Thandavan, K., Gandhi, S., Sethuraman, S., Rayappan, J. B. B., & Krishnan, U. M. (2011). Development and evaluation of a highly sensitive rapid response enzymatic nanointerfaced biosensor for detection of putrescine. *Analyst, 136*, 5234–5240.

Shen, L., Yang, L., & Peng, T. (1996). Amperometric determination of fish freshness by a hypoxanthine biosensor. *Journal of the Science of Food and Agriculture, 70*, 298–302.

Shi, G., Liu, M., Zhu, M., Zhou, T., Chen, J., Jin, L., et al. (2002). The study of nafion/xanthine oxidase/Au colloid chemically modified biosensor and its application in the determination of hypoxanthine in myocardial cells in vivo. *Analyst, 127*, 396–400.

Solanki, P. R., Kaushik, A., Agrawal, V., & Malhotra, B. D. (2011). Nanostructured metal oxide-based biosensors. *Asia Materials, 3*, 17–24.

Song, Y., Cui, K., Wang, L., & Chen, S. (2009). The electrodeposition of Ag nanoparticles on a type I collagen-modified glassy carbon electrode and their applications as a hydrogen peroxide sensor. *Nanotechnology, 20*, 105501.

Surendra, K. Y., Singh, J., Agarwal, V. V., & Malhotra, B. D. (2012). Nanostructured nickel oxide film for application to fish freshness biosensor. *Applied Physics Letters, 101*, 1–4.

Teng, Y. J., Chen, C., Zhou, C. X., Zhao, H. L., & Lan, M. B. (2010). Disposable amperometric biosensors based on xanthine oxidase immobilized in the Prussian blue modified screen-printed three-electrode system. *Science China chemistry, 53*, 2581–2586.

Thandavan, K., Gandhi, S., Sethuraman, S., Rayappan, J. B. B., & Krishnan, U. M. (2011). A novel nanostructured iron oxide-gold bioelectrode for hydrogen peroxide sensing. *Nanotechnology, 22*, 265505.

YuanJie, T., Chen, C., ChangXiang, Z., HongLi, Z., & MinBo, L. (2010). Disposable amperometric biosensors based on xanthine oxidase immobilized in the Prussian blue modified screen-printed three electrode system. *Science China Chemistry, 53*, 2581–2586.

Yu Febuxostat, K. (2007). A novel non-purine selective inhibitor of xanthine oxidase for the treatment of hyperuricemia in gout. *Recent Patents on Inflammation & Allergy Drug Discovery, 1*, 69–75.

Zhao, X., Cui, X., Di, L., & Li, W. (2002). Determination of hypoxanthine and xanthine in hippocampus by HPLC method. *Zhong Yao Cai, 25*, 716–717.